Available online at www.sciencedirect.com

ScienceDirect

journal homepage: www.elsevier.com/locate/bbe

Original Research Article

Initial clinical evaluation of image fusion based on rigid registration and supporting percutaneous liver tumor ablation

Dominik Spinczyk [a,*], *Marcin Stronczek* [a], *Aleksandra Badura* [a], *Piotr Sperka* [a], *Dorota Krywalska* [a], *Anna Wolinska* [a], *Agata Krason* [b], *Sylwester Fabian* [b], *Mateusz Bas* [b], *Andre Woloshuk* [c], *Jaroslaw Zylkowski* [d], *Grzegorz Rosiak* [d], *Dariusz Konecki* [d], *Krzysztof Milczarek* [d], *Olgierd Rowinski* [d], *Ewa Pietka* [b]

[a] *Evertop Sp. z o. o., Chorzów, Poland*
[b] *Silesian University of Technology, Faculty of Biomedical Engineering, Zabrze, Poland*
[c] *Purdue University, Weldon School of Biomedical Engineering, West Lafayette, IN, USA*
[d] *II Department of Radiology, Medical University of Warsaw, Warsaw, Poland*

ARTICLE INFO

Article history:
Received 26 February 2020
Received in revised form
1 June 2020
Accepted 9 July 2020
Available online 21 July 2020

Keywords:
US guided percutaneous liver tumor ablation
Intraoperative US image fusion
Image fusion evaluation
Automatic registration method
Image guided abdominal intervention
Image guided navigation

ABSTRACT

Purpose: The purpose of this article is to present and evaluate a proposed rigid registration method in the application of real-time fusion of pre-operative 3DCT images and intraoperative 2DUS images.

Methods: A universal hybrid automatic rigid registration method was proposed, which allows registration of preoperative contrast enhanced CT with intraoperative 2D ultrasound images (neither CEUS nor 3DUS is required), with the possibility of manual correction. The method is based on automatically detectable markers, clearly identified in preoperative CT images, and by optical position tracking system during the procedure. A two-step fusion accuracy assessment was used. The first stage, the initial fusion assessment, was carried out at the time of the procedure. The second, objective stage (the final fusion assessment) was carried out after the procedure, and was based on the image and location data collected during the procedure. The clinical evaluation of the method was performed on 20 patients.

Results: For IFA and for Fusion Stability Assessment evaluation steps the following results were obtained, respectively: no fusion disorder: 10, good overlay: 8, permanently wrong fusion: 2 and no fusion disorders: 8, short-term fusion disorders: 9, frequent fusion disorders:3. The RMSE descriptive statistics (presenting order: median (first quartile third quartile) [min max]) was 8.87 (6.46 12.76) [5.04 18.84] mm.

* *Corresponding author at*: Evertop Sp. z o. o., 1-3 Dluga, 41-506 Chorzów, Poland.
E-mail address: dspinczyk@evertop.pl (D. Spinczyk).

https://doi.org/10.1016/j.bbe.2020.07.005

Conclusion: The results are qualitatively comparable with results obtained in other independent research, quantitatively comparable in accuracy, achieving mostly better results in terms of preparation time consumed and operating in real time, which justifies the possible clinical usage of the proposed method.

1. Introduction

Percutaneous thermal ablation, also called percutaneous radiofrequency ablation (pRFA), is a minimally invasive procedure carried out with imaging guidance. It is a known method of radical treatment of small liver, kidney, and lung tumors, especially in non-resectable patients, and is included in many international guidelines (e.g. European Society of Medical Oncology and American Society of Clinical Oncology). The results of small tumor treatment are similar to those surgically managed, however with much lower complication rates [1]. Thermal ablation are procedures that require high precision in lesion localization, thus image fusion of ultrasound (US) imaging with Computed Tomography (CT) or Magnetic Resonance Imaging (MRI) is an important asset. This fusion imaging method is of interest to surgeons who perform pRFA in the treatment of liver tumors, because the real-time fusion of multimodal images can increase monitoring and confidence in aiming during the procedure and allows more accurate location of the lesions and more precise puncture [2].

Use of US imaging only does not provide any information about the safety margin during pRFA due to air bubbles created when performing ablation and limited visibility of the tumor. Enhancement of US using contrast is an alternative that increases the accuracy of navigation during the procedure. However, commercially available US contrast agents do not provide sufficient image enhancement duration to clearly visualize the obscure target damage during the pRFA procedure. In addition improper targeting in US image may occur when regenerative or dysplastic nodules around the low HCC within liver cirrhosis are present, appearing similar to the target lesion. Independent use of CT also has its own limitations. In particular, it requires more time, and exposes the patient to radiation. At the same time, there are difficulties with aiming at the lesion, as it requires finding the needle trajectory in a narrow field of view and large needle angles [3,4]. The utilization of US and MRI fusion in liver ablation was not considered due to the limitations including limited MR scanner availability, a small range of equipment (needles, catheters, etc.) on the market that can be used in a strong magnetic, slower MR imaging performance compared to ultrasound (US) and computed tomography (CT) scans, possible interference between MR and RF systems and the requirement of using an open MR systems for imaging in near real time during placing of the electrodes [5]. Therefore authors chose Ultrasound (US) and Computed Tomography (CT) image fusion.

Rigid fusion of US and CT imaging methods are commonly used during liver surgical procedures including pRFA aided with fusion of US and CT imaging from C-arm proposed by Rossi and colleagues (2019) [6] or supported with fusion of intraprocedural ultrasound (US) and contrast-enhanced cone-beam CT (CBCT) for small hepatocellular carcinoma (HCC) presented by Monfardinin et al. (2018) [7] resulting in registration accuracy of 7 mm. In other cases, electromagnetic trace-based US and CT fusion allows to perform real-time positioning of a 22-gauge needle in the liver as proposed by Bing et al. (2019) [8] showing precision of 8.5 mm. US and CT fusion utilizing non-rigid registration of images include, for example, a method proposed by Lee and colleagues (2011) [9] were 3D US and CT images were fused based on gradient information and anatomical features found in both modalities resulting in fiducial registration error, which given a configuration of the fiducials, can be used to estimate the target registration error (TRE), of 2.4 mm for vessels and surfaces of the liver.

Performing 3D to 2D registration presents a challenge for non-rigid objects [10]. The local deformation of shape in fusion of CT and US images requires finding correspondence in the content of the images usually on the basis of branching areas of the portal or hepatic veins [11]. As ablation procedure statistics indicate, liver tumors occur in all 8 of its anatomical segments [12], thus correspondence of points in the images of both modalities may not be provided in every location. Also, non-rigid registration of abdominal organs requires that the registration areas be limited to well-segmented organ masks, which were not available during surgery. To limit the high deformability of the liver, constraints, e.g. in shape space [13] need to be applied. Unfortunately, the changes in stiffness of the organ parenchyma depending on the lesions requires preparation of sets of shapes corresponding to the deformation of the organ for each patient separately. Additionally, fitting of CT volume to 2D US images can be considered a sparse data problem. The research carried out on marker-based registration of CT images of the patients' position during the ablation procedure showed that results of the Root Mean Square Error (RMSE) for rigid transformation is comparable with the outcome of using non-rigid transformations, e.g. Elastic Body Spline or Thin Plate Spline [14,15]. Hence, a hybrid method based on automatic rigid global matching with local rigid correction has been proposed.

The proposed method assumes that the deformation is a combination of 2 rigid transforms, limited to 2×6 degrees of freedom (two rigid transformations: one automatic, one manual) and is designed as a compromise to minimize the operator's necessary involvement, while sustaining accuracy. Limiting the number of degrees of freedom ensures greater reliability of fit, whilst reducing the duration of the process (with optional user input).

Previous ex-vivo study [16] allowed for pre-clinical evaluation of the system supporting diagnostics and therapy planning for percutaneous ablation of liver tumors. The study was two-part. Firstly, based on 20 patients CT scans of the abdomen, evaluation of the designed data acquisition protocol, evaluation of segmentation of organs and anatomical structures, planning of the therapy were performed. Next, system calibration, patient registration and fusion of the images were assessed by using a calibrated phantom. The average precision obtained for US probe calibration was 1.68 mm [16].

An in-vivo study of patients was carried out to assess the clinical value of this method in the presence of the aforementioned US challenges (safety margin problem, unclear nodule problem and confusing nodule problem).

The purpose of this article is to present and evaluate a proposed rigid registration method in the application of real-time fusion of pre-operative 3DCT images and intraoperative 2DUS images that do not require the visibility of a tumor lesion in both modalities and modification of transcutaneous liver tumor ablation.

2. Material and methods

The proposed method consists of the following step are presented in Fig. 1. Some detail could be find previously published work [16], where phantom evaluation has been performed.

The method for guidance used during liver tumor ablation works in real time, which provides the surgeon with immediate fusion of CT and US imaging and is also continuous throughout the ablation. Patients are anesthetized during the procedure, so significant movement of the patient's body is not a concern. The ablation needle is inserted based on synchronization with the respiratory phases. High-frequency ventilation methods, which can significantly reduce the respiratory amplitude, were also considered during this evaluation [17]. Unfortunately, use of such methods may increase the risk of baro-traumatic pneumothorax [18]. Considering that the mean age of the patients, was 62.9 years old and after medical consultation on the condition of patients, high-frequency ventilation method could not be used. In the beginning the markers, that are visible in CT examination and are recognized by the position tracking system, are attached to the patient's skin in order to allow further calibration.

Next, during the procedure, positions of placed markers are tracked using Claron Nav Hx40 [19] optical tracking system. The manufacturer ensures the calibration root mean square error at 0.2 mm. The image resolution of the camera is 1024 × 768px. Uniquely shaped markers, which were designed for this purpose by the author [20], are recognized by the camera and their 3D position can be calculated (Fig. 2). This provides a baseline for synchronization with respiratory phases. The problem of marker visibility in an optical tracking system has been solved by placing the tracking camera opposite to the operator. This placement of the camera provides a better view on both the US probe, ablation needle, and the patient's body surface. Anatomical positions of marker distribution are shown in Table 1.

In the first phase, an automatic method based on markers on the patient's abdominal surface detected by a position tracking system is used; the markers are also uniquely detectable in CT images. After the automatic phase, if necessary, a manual phase which uses the Horn global orientation algorithm to correct the automatic fit [21] is possible (Fig. 3). It should be noted that the verification of accuracy takes place in 3D on the basis of the mean square error of characteristic points marked in both imaging modalities by an expert, thus it can be concluded that the result has a lower tendency to underestimate the error value. It is possible to repeat the manual phase without the required accuracy being achieved.

The operation of the system involves performing multiple rigid registrations of misaligned coordinate systems assigned to the components i.e. CT image, patients position, US image, US probe to the frame of reference of the optical tracker (Fig. 3). The CT image frame is registered to the patients position with the use of markers recognized by the tracker and visible in CT image. The US image reference frame is registered to the

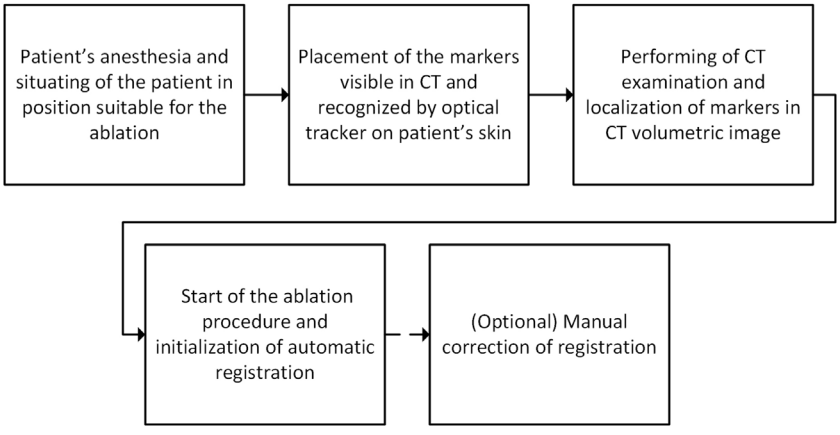

Fig. 1 – The steps of the proposed method of abdominal image fusion supporting percutaneous ablation based on rigid registration.

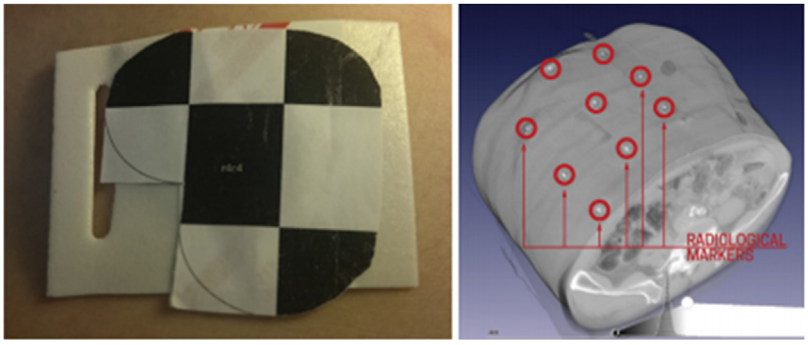

Fig. 2 – Image of markers that are used and their placement on patients skin.

probe's reference frame using a phantom of known geometry with elements visible in the US image. The average precision obtained for US probe calibration was 1.68 mm [16]. The US probe position and the patients position are calculated using markers. The conversion between subsequent coordinate systems allows the positioning of the CT and US image in the reference frame of the tracker.

The surgical conditions were developed based on the review of operational techniques and the need to take into account factors affecting organ deformation. The procedure takes place in a CT room. The patient remains anesthetized during CT examination (there were no respiratory synchronization protocols in the CT scanner used). The patient lies in the same position during the ablation procedure as during the tomography. For this reason it is not necessary to calculate the direction of gravitational force and organ deformations caused by gas insufflation (the procedure is performed percutaneously).

Intraprocedural steps are as follows: locating the patient and the model registration by automatically applying the algorithm for rigid adjustment of the image coordinate system to the patient's physical coordinate system (this step is repeated continually, for every marker's position obtained from the tracking system. The rigid transformation is updated multiple times per second), fusing the preprocedural CT and intraprocedural US image and the real-time image navigation during surgery.

Table 1 – Anatomical positions of skin markers.

Marker number	Anatomical location
1	Xiphoid process
2	Intersection of the midclavicular line and the right costal margin.
3	Intersection of the anterior axillary line and the right costal margin.
4	Intersection of the midclavicular line and the left costal margin.
5	Intersection of the anterior axillary line and the left costal margin.
7	Umbilicus

The registration method we propose is a hybrid method, which means that the design allows to work with any US head - the calibration method used is based on the open PLUS library [22], the method occurs in the first automatic phase, and does not assume the visibility of characteristic structures in fused images, it does not require the use of contrast enhanced US or 3D US imaging, the information about correspondence in the image content can be used in manual mode which acts as an amendment to the automatic mode. Manual mode includes the possibility of using expert knowledge in the form of indicating corresponding points in US and CT images. This option is in a separate application window presenting image fusions. The operator indicates the points corresponding in the US image and the corresponding 2D section. The operator has the ability to change the position and rotation of the CT cross-section in the x, y and z axes. If necessary, the fusion may be repeated multiple times in extremely difficult cases (after performing the manual correction, the additional transformation is combined with the automated one), as part of this method, an imaging protocol has been developed in which it is necessary to perform one 3D volume with contrast (at the exhalation phase).

The test is performed after sticking markers and the patient has been anesthetized, which ensures better repeatability of the respiratory cycle. This is performed using the respirator relative to imaging protocols used in radiotherapy, where the respiratory cycle is averaged during free breathing, and normally performs 10 volumes distributed linearly over the average respiratory cycle (0, 10, . . ., 90% respiratory phase). An optional concept could be developed in addition to the above approach: a protocol for performing 3D volume, opposite phase respiratory cycle acquisition. The goal of this method would be to determine the amplitude of respiratory movements of the pathological tissue, which allows for estimating mobility and narrowing down the search region for lesions using common 2D US imaging.

2.1. *Proposed fusion evaluation methods*

The correct fusion of images in various modalities (pre-surgery CT, mid-surgery CT, and mid-surgery US) is of key importance for the functioning of this system. Fusion errors result in

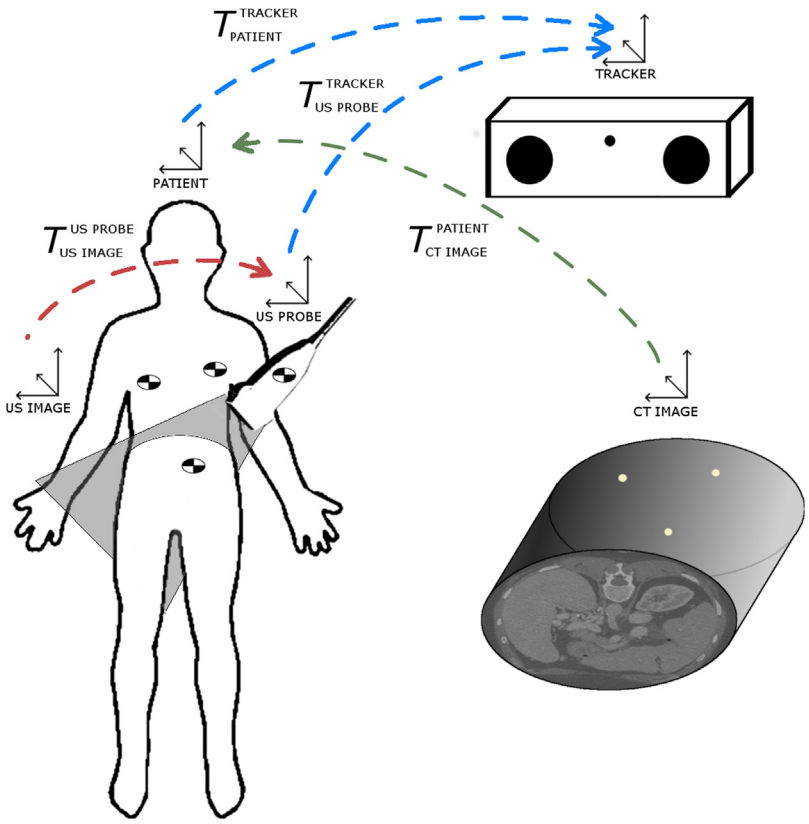

Fig. 3 – The schematic of transformation between reference frames of components forming the system.

navigation errors and, consequently, create a significant risk to the patient's health. This threat may come not only from the possibility of improper tool guidance, but also prolongation of the procedure itself. This method was validated with the use of a liver phantom [16]; with the consent of the Ethics Committee, research has been transferred from the phantom to the clinical environment. Given the above, we consider it highly desirable to verify the fusion on an artificial or animal model, particularly in CT.

A two-step fusion accuracy assessment is assumed: 1) First stage: the Initial Fusion Assessment (IFA) is carried out at the time of the procedure to determine the fusion quality for imaging modalities used during the procedure, 2) Second stage: the final Fusion Stability Assessment (FSA) is carried out after the procedure based on the image and location data collected during the procedure. This assessment consists of determining several coverage factors of the predicted and real model, based on the assessment of the radiologists. The nominal scale presented in the work, along with the significance of its individual values, was proposed by a team of radiologists with over 5 years of experience in percutaneous liver ablation surgery and is treated as an expert measure.

2.1.1. *Initial fusion quality assessment*

Initial Fusion Assessment is performed at the beginning of the procedure by radiologists experienced in percutaneous ablation. It assumes checking the quality of fusion using all imaging modalities provided for the procedure, i.e. US and CT of areas selected by the radiologists, including the focal change being the current target of the procedure. If more than one nodule is visible, the initial US assessment must apply to all of them. In the case of CT, the initial assessment of subsequent targets can be postponed to the next stage of the procedure, if imaging of all targets is not possible in a single CT scan.

IFA is carried out by the radiologists performing the procedure at the beginning, after the initialization of the system. For this assessment, we introduced a dedicated scale with the following points: very good fusion quality (IFA1), satisfactory fusion quality (IFA2), periodic problems with fusion, unsatisfactory quality (IFA3), incorrect initial fusion needing manual intraoperative correction (IFA4).

IFA 1 means the radiologists' statement of the correct overlapping of images from preprocedural examinations with intraprocedural images. IFA 2 means small, marginal, but not objectionable by the operator inaccuracy of image overlay. IFA 3 generally means good overlay of pre- and intraprocedural images with significant short-term system inaccuracies (suspensions, loss of purpose target) or a clear shift in direction and degree that the operator can compensate for visually. IFA 4 means a completely inaccurate fusion that has to be corrected in the navigation software during the procedure.

The aim of the initial assessment is to verify the correctness of the system's operation. Finding an erroneous fusion in any modality requires the technical team responsible for the correct operation of the system to take immediate action to

correct the error. A short time, specified by the operator, is allowed for making necessary corrections (several minutes).

2.1.2. *Final fusion assessment*

The system's stability, and the degree of coverage of the actual and system-calculated focal length position, is assessed after the procedure. For this assessment of fusion stability (FSA), a 3-point scale is employed: no fusion disorders (FSA 0), short-term fusion disorders not impeding navigation (FSA 1), frequent fusion disorders that significantly disturb or prevent the operator from perceiving the field correctly (FSA 2).

At the final stage of evaluation, a numerical measure is proposed. Two sets of corresponding points are arbitrarily selected in the US and CT images (minimum number of points was three; average was five). These points represent characteristic structures like veins, ligaments, gallbladder etc. which were marked if visible in both modalities. Next, Root Mean Square Error (RMSE) of chosen target points is employed resulting in Target Registration Error used to evaluate the calibration and patient position registration. It was defined as:

$$RMSE\,TRE = \sqrt{\frac{1}{N}}$$

where N was a number of selected points, x_i and y_i were the i-th marker positions in the first and second coordinate system, respectively. R and t were the rotation and translation matrices, respectively.

The rotation and translation matrices, representing a rigid transformation between the US image frame of reference and the corresponding CT slice, are calculated using Singular Value Decomposition (SVD) [23]. Assuming X and Y as sets of manually selected points in US and CT images respectively, we can calculate a covariance matrix W:

$$W = XY^T$$

Using SVD we can decompose W into:

$$SVD(W) = U\Sigma V^T$$

The rotation and translation matrices are calculated in the following way:

$$R = UV^T$$

$$T = \mu_X - R\mu_Y$$

where μ_X and μ_Y are centroids of selected point sets.

2.2. *Clinical material*

Over the course of this study, 20 patients (9 women, 11 men) underwent surgery using this system; mean age was 62.9 years (standard deviation 10.6, median 62). Reporting criteria included: 1) age, sex, and medical history of patient, 2) description of the procedure, 3) description of the visibility of structures in the images of both modalities, 4) significance and possible amplitude of the displacement of the tumor or other structure during respiratory, 5) motion in the US image, 6) initial fusion assessment and FSA on a numerical scale, 7) the Root Mean Square Error used as Target Registration Error measure.

Results of fusion quality assessment for cases were carried out by a team of three radiologists, each of which possessing over five years of experience in diagnosis and the minimally invasive therapy of pRFA procedures (ordinal values were agreed by the team, and numerical values were averaged from the evaluation carried out independently by individual persons).

The study was approved by the bioethics commission at the Medical University of Warsaw (KB/33/2018). Principles stated in Declaration of Helsinki on Ethical Principles for Medical Research Involving Human Subjects were followed.

3. Results

Table 2 presents the patient information and fusion quality measures.

Overall, a median distance of 8.87 mm was recorded. The first and third quartiles were 6.46 and 12.76 mm respectively. The greatest distance observed was 18.84 mm, with this case being considered the least satisfying result of all. The IFA was at level 4, meaning the US and CT images did not match; the FSA approached level 2, which means severe image fusion instability and disturbance. The shortest distance recorded was 5.04 mm, with this case being considered the best result. IFA was at level 2, meaning the mismatch of images was marginal; FSA was reported at level 0, showing no fusion instabilities. Unfortunately, no cases of IFA1 at level 1 were recorded.

Tables 3 and 4 present RMSE descriptive statistics broken down by the IFA and FSA values, respectively. The analysis showed that from the presented 20 cases, 10 US and CT image fusions retained the IFA measure at level 2, and 8 held FSA measure at level 0, meaning that no fusion distortions were noticed; in one case of stability a small, marginal, but not objectionable by the operator inaccuracy of image overlay was observed. In 8 patients IFA at level 3 was noticed; this means that a good overlay of pre- and intraprocedural images with significant short-term system inaccuracies (suspension, loss of purpose) or a clear shift in direction, and degree that the operator can compensate visually, was found. In 2 cases a completely permanent and wrong fusion was observed. In our study 9 cases of short-term fusion stability distortions which did not impede navigation (FSA 1) were noticed. FSA 2 was recorded in 3 patients. This meant that in both cases frequent fusion distortions that significantly disturbed or prevented the operator from perceiving the filed correctly were present.

The target lesions present in the liver were visible on both US and CT in 16 cases. When the lesion is visible in both modalities the registration outcome is the most reliable. In 2 cases, the hepatic lesion were only visible in US examination. Due to the patient's health state or possible allergic reaction, there was no possibility of using contrast enhancement. In other 2 cases lesions were not present in both the US and CT examination. Surrounding anatomical landmarks were used for assessing the registration quality of images.

Table 2 – Quantitative assessment of intraoperative US and preoperative CT fusion.

Patient ID	Gender	Age	Projection plane	RMSE TRE [mm]	Localization depth	IFA	FSA	Registration times [s]	Lesion visibility in US and CT	Annotation
1	F	71	transverse	12.84	Segment VI	IFA3	FSA1	139	–	A significant shift in the vertical axis of the US image was observed, insignificant in the horizontal axis.
2	F	62	frontal-like	6.14	Segment V	IFA2	FSA0	226	US and CT	A tumor clearly visible in both modalities, a good case for verifying fusion. The shift of CT-US images in the fusion is very slight (in the exhalation phase). The CT image compensates for the acoustic shadow that overrides the change in US examination.
3	M	77	transverse	14.26	Segment VII	IFA3	FSA1	244	US and CT	A thick layer of fat tissue, strongly pressed US probe.
4	M	77	transverse-like	12.53	Segment VIII	IFA3	FSA1	175	US	Poor visibility of structures in CT.
5	M	?	frontal	8	Segments II/IVa	IFA3	FSA0	211	US and CT	A clearly visible change in the CT modality. After making corrections, the structures overlap sufficiently.
6	M	63	transverse	8.1	Segment III	IFA3	FSA0	152	US and CT	Heterogeneous tumor in CT, visible cysts. Slight fusion images were observed. The CT image compensates for the acoustic shadow that obscures the change in US.
7	F	87	transverse-like	11.59	Segment VI/VII	IFA2	FSA1	116	US	Firmly pressed US probe to the abdomen.
8	M	63	transverse	18.84	Segments VI	IFA4	FSA2	330	–	Periodically, marker visibility was lost. Image coverage with slight shift in the vertical axis of the US image.
9	F	64	sagittal-like	10.53	Segment VI	IFA2	FSA0	106	US and CT	A clearly visible outline of the liver in both modalities. After correction, the coverage of the images is sufficient.
10	M	57	transverse	15.93	Segment VII	IFA4	FSA2	280	US and CT	Highly visible dishes and liver outline both in US and CT scans.
11	M	49	transverse	7.41	Segment II	IFA3	FSA1	196	US and CT	Image fusion is periodically unstable. After correction in 2 axes, the structures overlap satisfactorily.
12	M	59	transverse	8.78	Segments V/VIII	IFA2	FSA1	105	US and CT	Highly visible blood vessels. Adipose tissue was compressed to a depth of about 8 mm (based on the measurement of the thickness of subcutaneous fat) and intraperitoneal in CT and US in a similar location.

Table 2 (*Continued*)

Patient ID	Gender	Age	Projection plane	RMSE TRE [mm]	Localization depth	IFA	FSA	Registration times [s]	Lesion visibility in US and CT	Annotation
13	M	74	transverse-like	16.22	Segment VII	IFA3	FSA2	271	US and CT	Periodically unstable image. A visible lesion in USG and CT
14	F	43	transverse-like	6.075	Segment V	IFA2	FSA0	177	US and CT	Clearly visible cyst in both images, visible vessels in CT, US probe strongly pressed to the abdomen.
15	M	61	transverse	7.41	Segment II/III	IFA2	FSA1	121	US and CT	Visible vessels, USE Doppler was used. Moderately good coverage of structures.
16	F	52	transverse	5.7	Segment VIII	IFA2	FSA0	211	US and CT	Highly visible dishes in both modalities. After correction, the images overlap sufficiently, matching was possible due to the visibility of the change in both modalities. Fatty compression at level was observed 1 cm on US image in relation to CT.
17	F	73	frontal-like	11.19	Segment VII	IFA2	FSA0	146	US and CT	Highly visible dishes in both modalities. Images overlapped after slight correction to a satisfactory degree.
18	F	66	transverse-like	8.96	Segment V/VI	IFA3	FSA1	119	US and CT	After correction, the cyst coverage is correct.
19	F	52	transverse	5.04	Segment II	IFA2	FSA0	105	US and CT	The fusion is correct, the quality is satisfactory.
20	M	44	transverse	6.01	Segment VII/VIII	IFA2	FSA1	132	US and CT	The fusion is correct, the quality is satisfactory.

Table 3 – RMSE descriptive statistics for Initial Fusion Assessment levels (presenting order: counts, median, first-third quartile 15-, min, max).

Case group	Counts	Median (mm)	First quartile (mm)	Third quartile (mm)	Min (mm)	Max (mm)
Overall	20	8.87	6.46	12.76	5.04	18.84
IFA 2 – no fusion disorder	10	6.14	5.7	10.53	5.04	11.19
IFA 3 – good overlay	8	10.75	8.03	13.91	7.41	16.22
IFA 4 – permanently wrong fusion	2	17.39	16.66	18.11	15.93	18.84

Table 4 – RMSE descriptive statistics for Fusion Stability Assessment levels (presenting order: counts, mean, standard deviation, min, max).

Case group	Counts	Median (mm)	First quartile (mm)	Third quartile (mm)	Min (mm)	Max (mm)
Overall	20	8.87	6.46	12.76	5.04	18.84
FSA 0 – no fusion disorders	8	7.07	5.79	9.92	5.04	11.19
FSA 1 – short-term fusion disorders not impeding navigation	9	8.96	7.41	12.69	6.01	14.26
FSA 2 – frequent fusion disorders that significantly disturb prevent the operator from perceiving the field correctly	3	16.22	16.07	17.53	15.93	18.84

The times required for performing registrations are measured in the software. The time of automatic phase is calculated as period between initialization (user input) of the first phase and the successful result of registration.

The time of manual phase is measured from the starting of the phase (user input), throughout the selection of target points, until successfully performing registration by the software.

The duration of the first automatic phase is approximately 2 min; this is the time needed to assign unique labels to auto-detectable markers in CT, and is performed before the start of the procedure. The second manual phase takes approximately 3 min, on average; this requires entering a minimum of 3 pairs of corresponding points.

4. Discussion

Ablation of liver tumors is performed either percutaneously, laparoscopically or in open procedures. The operator faces different challenges in each of these techniques. From the point of view of invasiveness of the method, percutaneous techniques are the least invasive for the patient, at the same time the most difficult to localize the precisely damaged lesion in the intraoperative conditions by the operator. So we are dealing with a clinical compromise, which is decided by the operator, whether the application is more difficult less invasive technique or simpler more invasive. The work proposes a fusion technique supporting percutaneous technique.

In the developed method, a pre-operative image acquisition protocol, which is performed after complete anesthesia of the patient and is based on the respiration regulation by the ventilator and the patient's position during the procedure was proposed. This allows for maximum repeatability of biomechanical conditions for preoperative imaging with repeated surgery conditions. Below, the obtained results are more broadly referred to the work of other authors in relation to laparoscopic techniques, non-rigid registration, ablation validation and other related topics.

Similar study was presented by Kang et al. [24] where the usefulness of 3D CT-2D US virtual fusion on exhalation compared to real inspiration fusion was quantified. The 3D US imaging was used to generate the exhaled image. The 3D CT was performed on exhalation or on inhalation and exhalation (depending on the doctor's decision). In our method the fusion was carried out on the exhalation to compensates for breathing movements. Additionally, we did not use 3D US because many facilities (including those where tests were carried out), do not have an ultrasound to which the 3D US head can be attached. In addition, it is not possible to transmit 3DUS images in real time.

Direct comparison of results is not straightforward. Based on a literature review, the mean square registration error is commonly used as a measure of fusion evaluation, and the metric coincides with the RMSE error defined in the paper. On the other hand, no results were found corresponding to the nominal expert scale proposed in the work (Initial fusion quality assessment: IFA1, IFA2, IFA3, IFA4 and final fusion assessment: FSA 0, FSA 1, FSA 2), therefore the comparison is focused on the value of the registration error.

The results presented here are comparable with those obtained in other works. Wein W et al. [25] (point-based 9.7 mm, rigid 9.0 mm and affine registration 8.1 mm) proposed a method of US image simulation based on CT images and automatic registration method. Based on 25 patients, the author obtained a registration error at the median level of 8.1 mm with a range of 3.0–21.5 mm. In turn, Mauri et al. [26] (rigid) presented a single-plane automated method based on covering the vascular structure mask visible in both modalities which was tested on a group of 9 patients (6 males, 3 females; age range: 53–87, mean age: 68), scheduled for percutaneous thermal ablation of liver lesions, underwent CT–US fusion obtained using automatic registration. An error with median value of 6 mm was obtained.

In a publication from Tang and colleagues [27], a group of 77 patients achieved a success rate of 84%, defined as coverage of the planned zone before surgery with the ablation zone verified in CT after surgery. However, the fusion method required matching the content of US images based on the portal vein branch. The time required for fusion synchronization was on average 14 min (in the range of 5–55 min). Mauri et al. [12] showed ablation success in 90% of 295 cases; correct registration took from 5 to 20 minutes. A clinical evaluation of spatial accuracy of CT and Real-Time US fusion for imaging liver metastases was proposed Hakime et al. [28]. With the use of the volume-based fusion imaging system Vnav, and finding characteristic anatomical landmarks, the authors acquired a 7.05 mm registration distance. In AJ et al. (2019) [29] a comparison for usage of CT-US fusion fine needle aspiration with simple US guidance is presented. A Philips PercuNav Image Navigation system was used for performing image fusion. The resulting fusion fitness values were on average equal to 4.5 mm but it was required to repeat the registration process three times for 5 of patients, and this significantly extended the time it took to prepare the fusion.

Yamid et al. [30] proposed a hybrid semi-automatic registration method allowing to impose a biomechanical model on the laparoscopic image of the liver. The average registration error was about 10 mm, and the average time needed for registration was 5.56 min. The results of the method proposed in the article are slightly better in terms of accuracy and time consumed. Robu et al. [31] proposed a fast, global method for the initial rigid alignment between a 3D mesh derived from a preoperative CT of the liver and a surface reconstruction of the intraoperative scene. The authors only evaluated graphically the quantitative assessment of the proposed method on video films from laparoscopic liver resection. Referring to the obtained approx. 90% positive qualitative fusion validation (Table 2 18 of 20 cases, Table 3–17 of 20 cases) a good qualitative assessment of the proposed method can be found. Fusaglia eta al. [32] presented an approach for application in laparoscopic liver surgery, which reconstructs an intraoperative volume of the underlying intrahepatic vessels in real time through an ultrasound (US) sweep process. The authors obtained the average registration accuracy between preoperative 3D CECT and reconstructed 3D US of 7.2 mm in the left lobe and 9.7 mm in the right lobe of the liver. The average time required for performing the registration was 12 min. The results of the method proposed in the article are comparable in accuracy, and much better in terms of time consumed.

The IFA and FSA nominal scales for fusion assessment were introduced as an attempt to measure the operator's satisfaction. In the initial assessment of fusion, 10 out of 20 cases were classified as satisfactory (IFA2 - Table 2). In the final assessment of the fusion, 17 cases were classified as FSA0 and FSA 1 (Table 2). The final grade was better than the initial grade because it included the possibility of manual correction. Image fusion was classified as unsatisfactory in only 2 cases. Comparing our results with those of others, in the scope of quantitative assessment, this method (based on one or two rigid transformations) achieves comparable effects to other methods in this transformation class (8.87 mm vs 8.5 [8], 9.0 mm [25] and 11 mm [26]), while reducing significantly the time needed to complete registration (3 min vs 14 min [27], from 5 to 20 minutes [12]), while maintaining a level match success rate of 90% (90 % vs 84% [27] and 90% [12]). Non-rigid methods achieving better results require finding anatomical correspondence in the content of CT and US images (6.0 mm [26], 7.05 [28], 8.1 [25]), which is not possible in all locations where there are focal changes in the liver, and also significantly increases the duration of the procedure.

With regard to deformability of the liver during pRFA, the non-rigid registration of 2D US images from 3D CT is challenging. Due to the low signal-to-noise ratio and contrast in the ultrasonic image, reflection of organ and tissue boundaries, and acoustic shadows caused by hard structures of the rib arches it is difficult to track changes in shape [36]. We compared our study with non-rigid registration of images. Huang et al. [10] proposed a modification of non-rigid demons registration. No calculation time was given. The method was validated only graphically and qualitatively on images from one patient, so it is not possible to directly compare the results. Weia et al. [37] proposed a registration method which is focused on both, the vessel structures and the boundary of the liver segmented in US images using a 2D UNET architecture. Correct registration in the error range of 1–30 mm was obtained for 70% of images. The method can process from 2 to 5 frames per second. Our method has achieved comparable results and enables processing of 10–20 frames per second (restrictions are only due to the performance of marker tracking by the position tracking system - the declared time resolution of the ClaronNav Hx 40 is 20 frame per second) while not relying on the visibility of vascular structures in the image content. This is an advantage, especially when lesions are localized in any organ parenchyma and the 2D US projections show no vascular structures.

As for validation of outcomes after the pRFA procedure, Pohlman et al. [3] proposed a fusion method for validation of the ablation area using a rigid and affine transformation composite, based on the visibility of the ablation needle in both ultrasound and CT images. Cazoulat et al. [38] proposed a method of registering CT images taken before and after surgery using a biomechanical model of the liver, additionally using information about the displacement of vascular structures. Hendriks et al. [39] used a semi-automatic 3D CT registration method before and after surgery to predict the development of cancer. Kanoulas et al. [40] enhanced the 2D US head scanning method, by taking a few minutes to obtain a map of vascular structures in a static 3D image of the scanned organ. In another work, Luu et al. [2] proposed a method for registering pre-treatment 3D CECT with intra-operative 3D CT without contrast enhanced. With regard to the proposed method, this work is beyond our scope, as the presented method supports the earlier stage of introducing the ablation needle on the basis of preoperative CT, where the needle is not visible. In addition, in the facility where evaluations were carried out, radiologists do not insert the needle in the ultrasound image plane (using a biopsy attachment), which means that the entire needle is also not visible in ultrasound images. As in the case of works [38,39], we do not perform CT after surgery. A method of predicting early tumor recurrence after ablation based on the radiomical features of 3D CECT images after surgery was proposed by Yuan et al. [41]. That

approach supports further patient diagnostics and can be treated as a supplement to the proposed approach. Referring to work [40] static scanning does not capture dynamic changes in the shape of the liver during breathing. In addition, CEUS enhances the visibility of the pathology for 1–2 seconds, so it is not used in all facilities to support pRFA. In reference to the work [2], the proposed method did not use intraoperative CT images or CECT-CT fusion. Independent work is underway on the effective selection of an ablative antenna. Lee et al. proposed a thin coaxial antenna with a better absorption coefficient [42]. Gas [43] proposed a method of structure optimization of multi-slot coaxial antennas to get the best impedance matching with the treated tissue.

When considering the limitations of our study, most prominent of these would be the small subject group (20 patients); a larger study is needed to clearly assess a quality measure of the proposed method. It is worth noting, however, that our method was designed to be universal to any type of US probe - the probe grip is adjustable, and the calibration procedure is the same overall (this makes the approach applicable to most US machines typically used in the hospital environment). The fusion itself was performed by 3 coordinators. Also, an advantage of our study was the fact that the fusion assessment was performed immediately after the procedure, instead of in a retrospective manner.

Furthermore, a robust method of determining characteristic points on US images should be implemented. Search for the points should be based on clearly visible lesions, places of bifurcation of the vessels, and not points on the surface of the liver, for example, the shape of which may change during the procedure and under compression of the US probe. Preparation of the patient before the procedure takes very little time, and does not require corrections. In future it may be possible to reduce the amount of time required to transfer CT data from scanner to workstation.

The more superficial changes, i.e. closer to the US probe, imaged especially on cross sections, showed the highest fusion accuracy. In future, focus should be placed on obtaining the maximum overlap of CT and US images in the area of deeply located changes, also. In our opinion, ad hoc improvement in coverage can be achieved by making adjustments that consider image shift resulting from compression of body shells with an US probe. Perhaps extending the duration and adding other methods of acquisition of US images would be worthwhile, in order to increase the amount of available video material.

As mentioned previously, the high-frequency ventilation respiratory support allows for better control of the respiratory motion. It reduces the amplitude of breathing signal and lowers the overall dose-length product compared with conventional ventilation used during estimation of breathing motions with CT scanning [17]. Because of this, it finds application in surgery guiding techniques. However, this method cannot be used for patients with Chronic Obstructive Pulmonary Disease, obesity or recent pneumothorax. It carries also a higher risk of causing barotraumatic pneumothorax. Considering that the average age of the patient group was 62.9 years old, use of high-frequency jet ventilation was contraindicated. Future research in this field is needed.

Localization of the needle tip is a crucial task that increases the overall performance of computer aided pRFA. Due to subcutaneous fat, severe cirrhosis and fatty liver the inserted ablation needle is obscured or when changing the position of the needle, because of previous ablation zone, the needle becomes invisible to the operator. It is impossible to perform the puncture when the information about obstacles like vessels or the gallbladder in the way of the needle is lacking [44]. Sometimes the tip of the bipolar electrode may be unclear in B-mode US imaging [45]. According to studies of biopsy procedures, deflection of needle may occur [46]. Therefore, further studies should account for localization of the pRFA needle in US images to study the precision of insertion of the needle into the target lesion.

5. Conclusion

The method for evaluation of preprocedural 3D CT and intraprocedural 2D US image fusion for support of percutaneous liver tumor ablation was presented. The primary focus of this research was to evaluate the in-vivo performance of the previously proposed fusion method for supporting pRFA procedures. Use of rigid registration method allowed real-time 2D US and 3D CT image fusion with any 2D US probe (neither CEUS nor 3DUS is required).

The next step is to evaluate percutaneous ablation on a wider group of patients, with follow-up of and analysis for cancer recurrences in correlation with coverage ratio of tumor volume by an ablative lodge. In more complex methodology, the developed method can be treated as a good initialization of deformation methods, while it is refreshed several times per second in real time during the procedure.

Clinical research on application of proposed method to other organs is needed. A potential use for kidney interventions, providing less risk of damaging structures such as renal vessels, renal pelvis, adrenal glands, spleen and colon due to the tracking of the needle path, or for the less visible tail of the pancreas is substantial. Consideration should be given to the displacement of the entire organ, relative to the lying hollow organs, due to the pressure of the ultrasound head.

Furthermore, taking into account a patients group of younger age, high-frequency jet ventilation should be applied to decrease the respiratory motion amplitude, thus possibly leading to better registration results.

Funding

Presented results were obtained in the project, ''System for computer aided diagnosis and minimally invasive therapy of abdominal cancer'' co-financed by the European Union, European Regional Development Fund. Institution granting funds: The National Centre for Research and Development – ncbr.gov.pl.

Declarations of interest

None.

CRediT authorship contribution statement

Dominik Spinczyk: Funding acquisition, Supervision, Conceptualization, Methodology, Writing - original draft, Writing - review & editing. **Marcin Stronczek:** Funding acquisition, Supervision, Software. **Aleksandra Badura:** Software, Data curation, Resources. **Piotr Sperka:** Software. **Dorota Krywalska:** Validation. **Anna Wolinska:** Validation. **Agata Krason:** Investigation. **Sylwester Fabian:** Investigation. **Mateusz Bas:** Investigation, Writing - original draft, Writing - review & editing. **Andre Woloshuk:** Writing - review & editing. **Jaroslaw Zylkowski:** Validation. **Grzegorz Rosiak:** Validation. **Dariusz Konecki:** Validation. **Krzysztof Milczarek:** Validation. **Olgierd Rowinski:** Validation. **Ewa Pietka:** Supervision.

Acknowledgements

The study was approved by the bioethics commission at the Medical University of Warsaw (KB/33/2018).

REFERENCES

[1] Viganò L, Laurenzi A, Solbiati L, Procopio F, Cherqui D, Torzilli G. Open liver resection, laparoscopic liver resection, and percutaneous thermal ablation for patients with solitary small hepatocellular carcinoma (≤30 mm): review of the literature and proposal for a therapeutic strategy. Dig Surg 2018;35:359–71. http://dx.doi.org/10.1159/000489836

[2] Luu HM, Klink C, Niessen W, Moelker A, Van Walsum T. Non-rigid registration of liver CT images for CT-guided ablation of liver tumors. PLoS One 2016;11. http://dx.doi.org/10.1371/journal.pone.0161600

[3] Pohlman RM, Turney MR, Wu PH, Brace CL, Ziemlewicz TJ, Varghese T. Two-dimensional ultrasound-computed tomography image registration for monitoring percutaneous hepatic intervention. Med Phys 2019;46: 2600–9. http://dx.doi.org/10.1002/mp.13554

[4] D'Onofrio M, Beleù A, Gaitini D, Corréas JM, Brady A, Clevert D. Abdominal applications of ultrasound fusion imaging technique: liver, kidney, and pancreas. Insights Imaging 2019;10. http://dx.doi.org/10.1186/s13244-019-0692-z

[5] Kelekis AD, Terraz S, Roggan A, Terrier F, Majno P, Mentha G, et al. Percutaneous treatment of liver tumors with an adapted probe for cooled-tip, impedance-controlled radio-frequency ablation under open-magnet MR guidance: initial results. Eur Radiol 2003;13:1100–5. http://dx.doi.org/10.1007/s00330-003-1847-2

[6] Rossi D, Bonomo G, Della Vigna P, Monfardini L, Orsi F, Solbiati L, et al. The role of ultrasound and cone beam CT fusion for guidance of thermal liver ablation; 2019.

[7] Monfardini L, Orsi F, Caserta R, Sallemi C, Della Vigna P, Bonomo G, et al. Ultrasound and cone beam CT fusion for liver ablation: technical note. Int J Hyperthermia 2018;35:500–4. http://dx.doi.org/10.1080/02656736.2018.1509237

[8] Bing F, Vappou J, Breton E, Enescu I, Garnon J, Gangi A. Accuracy of a CT-Ultrasound fusion imaging guidance system used for hepatic percutaneous procedures. J Vasc Interv Radiol 2019;30:1013–20. http://dx.doi.org/10.1016/j.jvir.2018.11.034

[9] Lee D, Nam WH, Lee JY, Ra JB. Non-rigid registration between 3D ultrasound and CT images of the liver based on intensity and gradient information. Phys Med Biol 2011;56:117–37. http://dx.doi.org/10.1088/0031-9155/56/1/008

[10] Huang S, wu K, Meng X, Li C. Non-rigid registration method between 3D CT liver data and 2D ultrasonic images based on demons model; 2019;1–15.

[11] Lee JY, Choi BI, Chung YE, Kim MW, Kim SH, Han JK. Clinical value of CT/MR-US fusion imaging for radiofrequency ablation of hepatic nodules. Eur J Radiol 2012;81:2281–9. http://dx.doi.org/10.1016/j.ejrad.2011.08.013

[12] Mauri G, Cova L, De Beni S, Ierace T, Tondolo T, Cerri A, et al. Real-time US-CT/MRI image fusion for guidance of thermal ablation of liver tumors undetectable with US: results in 295 cases. Cardiovasc Intervent Radiol 2015. http://dx.doi.org/10.1007/s00270-014-0897-y

[13] Luthi M, Gerig T, Jud C, Vetter T. Gaussian process morphable models. IEEE Trans Pattern Anal Mach Intell 2018;40:1860–73. http://dx.doi.org/10.1109/TPAMI.2017.2739743

[14] Spinczyk D, Zyklowski J, Wroblewski T. Continuous registration based on computed tomography for breathing motion compensation. Videosurgery Other Miniinvasive Tech 2013;8:265–72. http://dx.doi.org/10.5114/wiitm.2013.39505

[15] Spinczyk D. Image-based guidance of percutaneous abdomen intervention based on markers for semi-automatic rigid registration. Videosurgery Other Miniinvasive Tech 2014;4:531–6. http://dx.doi.org/10.5114/wiitm.2014.45048

[16] Spinczyk D, Badura A, Sperka P, Stronczek M, Pycinski B, Juszczyk J, et al. Supporting diagnostics and therapy planning for percutaneous ablation of liver and abdominal tumors and pre-clinical evaluation. Comput Med Imaging Graph 2019101664. http://dx.doi.org/10.1016/J.COMPMEDIMAG.2019.101664

[17] Denys A, Lachenal Y, Duran R, Chollet-Rivier M, Bize P. Use of high-frequency jet ventilation for percutaneous tumor ablation. Cardiovasc Intervent Radiol 2014;37:140–6. http://dx.doi.org/10.1007/s00270-013-0620-4

[18] Puijk RS, Ruarus AH, Scheffer HJ, Vroomen LGPH, van Tilborg AAJM, de Vries JJJ, et al. Percutaneous liver tumour ablation: image guidance, endpoint assessment, and quality control. Can Assoc Radiol J 2018;69:51–62. http://dx.doi.org/10.1016/j.carj.2017.11.001

[19] Claron Nav Hx40 - specification n.d. https://www.claronav.com/microntracker/microntracker-specifications/.

[20] Spinczyk D. Marker and method for automatic positioning of a patient, preferably in the image navigation systems. PL 406230, Polish Patent Office, June 8, 2015.

[21] Horn BKP, Hilden HM, Negahdaripourt S. Closed-form solution of absolute orientation using orthonormal matrices. Vol. 5; 1988.

[22] Lasso A, Heffter T, Rankin A, Pinter C, Ungi T, Fichtinger G. PLUS: open-source toolkit for ultrasound-guided intervention systems. IEEE Trans Biomed Eng 2014;61: 2527–37. http://dx.doi.org/10.1109/TBME.2014.2322864

[23] Marden S, Guivant J. Improving the performance of ICP for real-time applications using an approximate nearest neighbour search. Australas Conf Robot Autom ACRA 2012.

[24] Kang TW, Lee MW, Cha DI, Park HJ, Park HJ, Bang WC, et al. Usefulness of virtual expiratory CT images to compensate for respiratory liver motion in ultrasound/CT image fusion:

a prospective study in patients with focal hepatic lesions. Korean J Radiol 2019;20:225–35. http://dx.doi.org/10.3348/kjr.2018.0320

[25] Wein W, Brunke S, Khamene A, Callstrom MR, Navab N. Automatic CT-ultrasound registration for diagnostic imaging and image-guided intervention. Med Image Anal 2008;12:577–85. http://dx.doi.org/10.1016/j.media.2008.06.006

[26] Mauri G, De Beni S, Forzoni L, D'Onofrio S, Kolev V, Lagana MM, et al. Virtual navigator automatic registration technology in abdominal application. 2014 36th Annu Int Conf IEEE Eng Med Biol Soc EMBC 2014;2014:5570–4. http://dx.doi.org/10.1109/EMBC.2014.6944889

[27] Tang H, Tang Y, Hong J, Chen T, Mai C, Jiang P. A measure to assess the ablative margin using 3D-CT image fusion after radiofrequency ablation of hepatocellular carcinoma. HPB 2015;17:318–25. http://dx.doi.org/10.1111/hpb.12352

[28] Hakime A, Deschamps F, De Carvalho EGM, Teriitehau C, Auperin A, De Baere T. Clinical evaluation of spatial accuracy of a fusion imaging technique combining previously acquired computed tomography and real-time ultrasound for imaging of liver metastases. Cardiovasc Intervent Radiol 2011;34:338–44. http://dx.doi.org/10.1007/s00270-010-9979-7

[29] AJ L, Kalra N, Bhatia A, Srinivasan R, Gulati A, Kapoor R, et al. Fusion image–guided and ultrasound-guided fine needle aspiration in patients with suspected hepatic metastases. J Clin Exp Hepatol 2019;9:547–53. http://dx.doi.org/10.1016/j.jceh.2019.01.003

[30] Yamid E, Özgür E, Calvet L, Le Roy B, Buc E, Bartoli A. Combining visual cues and interactions for 3D-2D registration in liver laparoscopy; 2020;3–6. http://dx.doi.org/10.1007/s10439-020-02479-z

[31] Robu MR, Ramalhinho J, Thompson S, Gurusamy K, Davidson B, Hawkes D, et al. Global rigid registration of CT to video in laparoscopic liver surgery. Int J Comput Assist Radiol Surg 2018;13:947–56. http://dx.doi.org/10.1007/s11548-018-1781-z

[32] Fusaglia M, Tinguely P, Banz V, Weber S, Lu H. A novel ultrasound-based registration for image-guided laparoscopic liver ablation. Surg Innov 2016;23:397–406. http://dx.doi.org/10.1177/1553350616637691

[36] Che C, Mathai TS, Galeotti J. Ultrasound registration: a review. Methods 2017;115:128–43. http://dx.doi.org/10.1016/j.ymeth.2016.12.006

[37] Weia W, Xub H, Alpersa J, Tianbaob Z, Wangb L, Marko R, et al. Fast registration for liver motion compensation in ultrasound guided navigation. 2019 IEEE 16th Int Symp Biomed Imaging (ISBI 2019) 2019;1132–6.

[38] Cazoulat G, Elganainy D, Anderson BM, Zaid M, Park PC, Koay EJ, et al. Vasculature-driven biomechanical deformable image registration of longitudinal liver cholangiocarcinoma computed tomographic scans. Adv Radiat Oncol 2019;1–10. http://dx.doi.org/10.1016/j.adro.2019.10.002

[39] Hendriks P, Noortman WA, Baetens TR, Van Erkel AR, Van Rijswijk CSP, Van Der Meer RW, et al. Quantitative volumetric assessment of ablative margins in hepatocellular carcinoma: predicting local tumor progression using nonrigid registration software. J Oncol 2019;2019. http://dx.doi.org/10.1155/2019/4049287

[40] Kanoulas E, Butler M, Rowley C, Voulgaridou V, Diamantis K, Duncan WC, et al. Super-resolution contrast-enhanced ultrasound methodology for the identification of in vivo vascular dynamics in 2D. Invest Radiol 2019;54:500–16. http://dx.doi.org/10.1097/RLI.0000000000000565

[41] Yuan C, Wang Z, Gu D, Tian J, Zhao P, Wei J, et al. Prediction early recurrence of hepatocellular carcinoma eligible for curative ablation using a Radiomics nomogram. Cancer Imaging 2019;19:1–12. http://dx.doi.org/10.1186/s40644-019-0207-7

[42] Lee M, Son T. Helical slot antenna for the microwave ablation. Int J Antennas Propag 2019;2019. http://dx.doi.org/10.1155/2019/2126879

[43] Gas P. Optimization of multi-slot coaxial antennas for microwave thermotherapy based on the S11-parameter analysis. Biocybern Biomed Eng 2017;37:78–93. http://dx.doi.org/10.1016/j.bbe.2016.10.001

[44] Tomonari A, Tsuji K, Yamazaki H, Aoki H, Kang JH, Kodama Y, et al. Feasibility of the virtual needle tracking system for percutaneous radiofrequency ablation of hepatocellular carcinoma. Hepatol Res 2013;43:1352–5. http://dx.doi.org/10.1111/hepr.12096

[45] Hirooka M, Koizumi Y, Imai Y, Ochi H, Nakamura Y, Yoshida O, et al. Assessment of a needle-tracking system for bipolar radiofrequency ablation. J Med Ultrason (2001) 2016;43:185–91. http://dx.doi.org/10.1007/s10396-015-0679-4

[46] Li ADR, Plott J, Chen L, Montgomery JS, Shih A. Needle deflection and tissue sampling length in needle biopsy. J Mech Behav Biomed Mater 2020;104103632. http://dx.doi.org/10.1016/j.jmbbm.2020.103632